GEOLOGY | THE GEOLOGICAL SOCIETY OF AMERICA®

https://doi.org/10.1130/G46792.1

Manuscript received 6 July 2019
Revised manuscript received 28 September 2019
Manuscript accepted 1 October 2019

Published online 28 October 2019

Reef-flat and back-reef development in the Great Barrier Reef caused by rapid sea-level fall during the Last Glacial Maximum (30–17 ka)

Kazuhiko Fujita[1,2], Noriko Yagioka[2], Choko Nakada[2], Hironobu Kan[3], Yosuke Miyairi[4], Yusuke Yokoyama[4] and Jody M. Webster[5]

[1]Department of Physics and Earth Sciences, Faculty of Science, and Tropical Biosphere Research Center, University of the Ryukyus, 1 Senbaru, Nishihara, Okinawa 903-0213, Japan
[2]Physics and Earth Sciences Course, Graduate School of Engineering and Science, University of the Ryukyus, 1 Senbaru, Nishihara, Okinawa 903-0213, Japan
[3]Graduate School of Integrated Sciences for Global Society, Kyushu University, 744 Motooka, Nishi-ku, Fukuoka 819-0395, Japan
[4]Atmosphere and Ocean Research Institute, and Department of Earth and Planetary Sciences, The University of Tokyo, 5-1-5 Kashiwanoha, Kashiwa 277-8564, Japan
[5]Geocoastal Research Group, School of Geosciences, The University of Sydney, Sydney, New South Wales 2006, Australia

ABSTRACT

Reef growth patterns and the development of associated environments have been extensively studied from reef deposits from Holocene and previous interglacial highstands. However, reefs that grew during glacial lowstands are comparatively poorly understood. Here we show the formation of reef-flat and back-reef environments following rapid sea-level fall (15–20 mm yr^{-1} and 20–40 m in magnitude) during the Last Glacial Maximum (LGM) on the present shelf edge of the Great Barrier Reef. Sedimentological and foraminiferal analyses of unconsolidated reef sediments recovered in cores 111–140 m below sea level at Hydrographers Passage during Integrated Ocean Drilling Project (IODP) Expedition 325 reveal the occurrence of a benthic foraminiferal assemblage dominated by the genera *Calcarina* and *Baculogypsina*, which is common in modern reef-flat and back-reef environments in the Great Barrier Reef and elsewhere. This assemblage is associated with higher foraminiferal proportions in reef sediments and higher proportions of well-preserved *Baculogypsina* tests in the same intervals, which also characterize reef-flat environments. Radiocarbon (^{14}C–accelerator mass spectrometry) ages of reef-flat dwelling foraminifers (n = 22), which indicate the time when these foraminifers were alive, are consistent with the timing of the two-step sea-level fall into the LGM as defined by the previously published well-dated coralgal record. This foraminiferal evidence suggests the development of geomorphically mature fringing reefs with shallow back-reef lagoons during the LGM. Our results also imply that back-reef sediment accumulation rates during the LGM lowstand were comparable to those during the Holocene highstand.

INTRODUCTION

Reef growth patterns during interglacial sea-level highstands have been well studied based on drilling of Holocene and last-interglacial reef deposits (Montaggioni, 2005; Woodroffe and Webster, 2014). Reef growth has been characterized by three main patterns: "keep up", "catch up", and "give up", in addition to "prograded" and "backstepped" (Woodroffe and Webster, 2014; Camoin and Webster, 2015). In keep-up or catch-up mode, as reefs accrete vertically toward the sea surface, reef geomorphic zonation such as reef flat, back-reef lagoon, and fore-reef slope has been established. The accommodation space of a back-reef lagoon is gradually filled with transported reef-flat sediments as a result of wave action on exposed reef flats (e.g., Kennedy and Woodroffe, 2002; Smithers, 2011). Recently, reef growth patterns during the last-deglacial sea-level rise have been revealed (Camoin et al., 2012). However, reef growth patterns during glacial sea-level fall and glacial sea-level lowstands are yet to be fully understood (e.g., Esat and Yokoyama, 2006).

During relative sea-level (RSL) fall due to eustasy, glacio-hydroisostasy, and/or tectonic uplift, an emergent give-up type reef typically occurs (Woodroffe and Webster, 2014; Camoin and Webster, 2015). Depending on the rate and magnitude of the RSL fall and available substrate, the reef system progrades (migrates seaward) and a new reef develops at a lower elevation ("turn-on"), but as a consequence, the entire preexisting reef is left stranded ("turn-off"). Typical examples are reef flats during the late Holocene sea-level fall, when highly productive coral reef flats changed to less-productive rubble and algal flats (e.g., Smithers, 2011; Harris et al., 2015). Rapid tectonic uplift can also cause similar back-reef turn-off and the turn-on of a new reef in a more seaward position (e.g., Webster et al., 1998). However, little is known about how reefs and associated environments respond to more rapid and larger-amplitude sea-level falls.

Last Glacial Maximum (LGM) reefs have been observed at Mayotte (Indian Ocean), Vanuatu, Solomon Islands, Marquesas Islands (Pacific Ocean) (reviewed by Montaggioni, 2005), and Ryukyu Islands (Japan) (Sasaki et al., 2006) as thin veneers or coral communities 2–3 m thick, at depths of mostly 100–150 m below sea level (mbsl). More recently, sediment cores recovered from the shelf edge of the Great Barrier Reef during Integrated Ocean Drilling Project (IODP) Expedition 325 revealed that drowned

CITATION: Fujita, K., et al., 2020, Reef-flat and back-reef development in the Great Barrier Reef caused by rapid sea-level fall during the Last Glacial Maximum (30–17 ka): Geology, v. 48, p. 39–43, https://doi.org/10.1130/G46792.1

shelf-edge reefs composed of *in situ* coralgal frameworks and associated microbialites developed during the LGM and the subsequent last deglaciation (Webster et al., 2018; Braga et al., 2019; Humblet et al., 2019). In addition, combined paleo–water depths and >580 radiometric ages of the coralgal assemblages revealed a two-step sea-level plunge, each of several tens of meters in magnitude and a change rate of 15–20 mm yr^{-1}, into the LGM (Yokoyama et al., 2018). In response to these sea-level changes, five reef sequences have migrated vertically and laterally since 30 ka (Webster et al., 2018). Foraminiferal assemblages from unconsolidated reef sediments in the IODP Expedition 325 cores have also closely tracked associated changes in depositional environments. In particular, shallowing-upward sequences observed in the LGM deposits are likely related to the two-step falls in sea level (Yagioka et al., 2019).

Here we show the formation of reef-flat and back-reef environments following rapid sea-level fall (at a rate of 15–20 mm yr^{-1} and magnitude of several tens of meters) during the LGM on what is now the Great Barrier Reef shelf edge, based on benthic foraminiferal assemblages, abundances, and taphonomic grades combined with radiocarbon dating of foraminiferal tests. We propose a model of reef growth, including reef-flat and back-reef generation, in response to rapid sea-level falls during the LGM.

MATERIALS AND METHODS

A total of 65 unconsolidated sediment samples were collected at depths from 111 to 140 mbsl from six cores retrieved from inner and outer submerged reef terraces along two transects (HYD-01C and HYD-02A; Fig. 1) from Hydrographers Passage (19.667°S, 150.417°E). The grain-size composition and benthic foraminiferal taxonomic composition data for 47 of the 65 samples have been reported by Yagioka et al. (2019); 18 additional samples were analyzed for those data types in this study. For each sample, sediments were washed, dry sieved, and weighed (weight percent) to estimate grain-size composition. Sediments of 2–0.5 mm size fraction were split with a splitter until a subsample contained >150 benthic foraminifer tests. All benthic foraminiferal specimens were picked from the subsample, identified to the lowest taxonomic level possible, and counted. More than 500 particles in another subsample were identified and counted to estimate bioclast compositions for each sample. Preservation states of >100 tests of *Baculogypsina sphaerulata* picked from an additional subsample were categorized in each sample, mainly based on abrasion states of spines (the number of spines remained), into grade S (all spines remaining), grade A (some spines remaining), grade B (the roots of spines remaining), and grade C (no spines or roots remaining). The proportion of stained tests of *B. sphaerulata*, which indicates reworking from exposed older deposits (Yordanova and Hohenegger, 2002), was also calculated among >100 *Baculogypsina* tests in each sample. ^{14}C ages were measured on well-preserved tests (grades S, A, and B) of *B. sphaerulata* and *Calcarina* spp. from 22 selected samples (10–15 specimens for each sample). Accelerator mass spectrometry (AMS) analyses were performed using a single-stage AMS at the Atmosphere and Ocean Research Institute at the University of Tokyo (Japan). Conventional ^{14}C ages were calibrated to calendar ages using OxCal v.4.3 (https://c14.arch.ox.ac.uk/oxcal.html) using the Marine13 curve (Reimer et al., 2013).

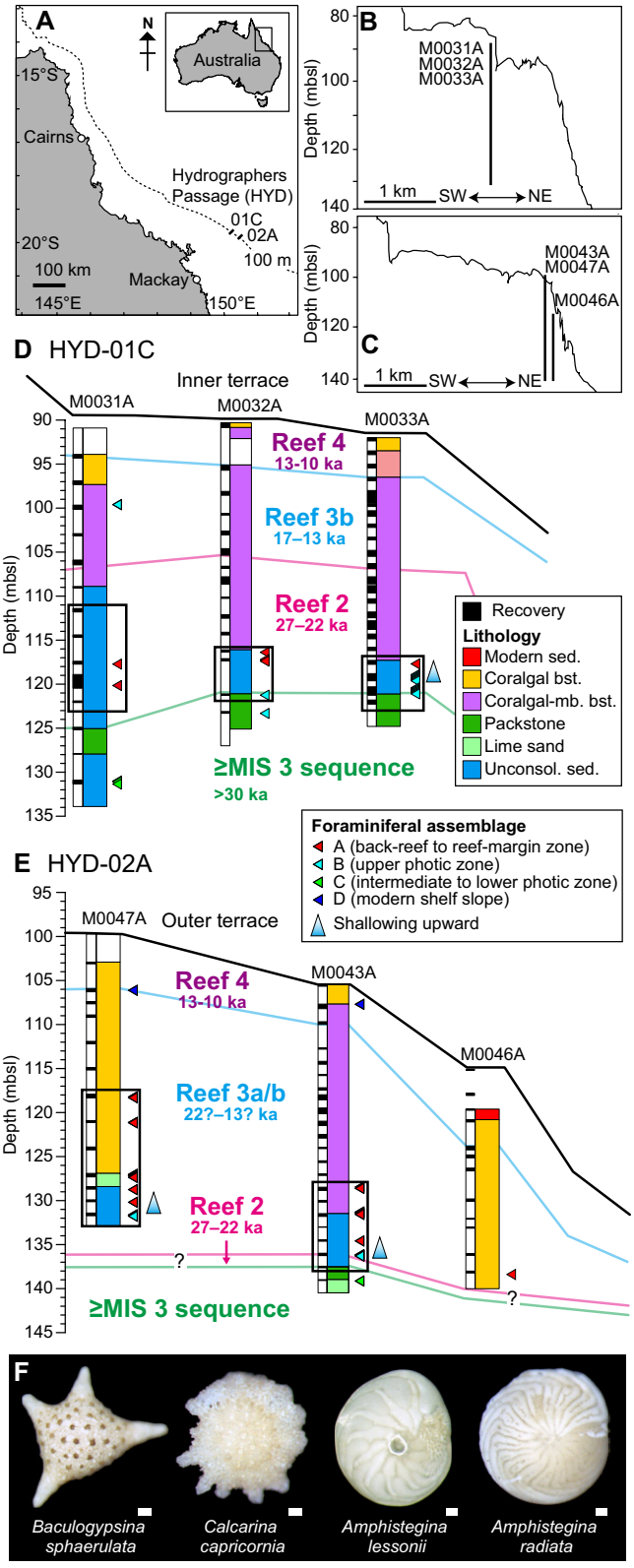

Figure 1. (A) Map of study area showing location of two transects at Hydrographers Passage (HYD), Great Barrier Reef. Dotted line indicates a 100 m depth contour line, corresponding to the continental shelf break. (B,C) Topographic profiles of two transects, HYD-01C (B) and HYD-02A (C), showing location of drill sites (after Hinestrosa et al., 2016). The numbers shown next to drill traces indicate hole numbers of the Integrated Ocean Drilling Project Expedition 325. (D,E) Lithostratigraphy and stratigraphic distribution of foraminiferal assemblages (Webster et al., 2018; Yagioka et al., 2019), showing core depth intervals examined in this study (black rectangles) for HYD-01C (D) and HYD-02A (E). sed.—sediment; bst.—boundstone; mb.—microbialite; Unconsol.—unconsolidated. mbsl—meters below sea level; MIS—Marine Isotope Stage. (F) Four key taxa of benthic foraminifers, which characterize assemblages A (*Baculogypsina sphaerulata* and *Calcarina capricornia*) and B (*Amphistegina lessonii* and *Amphistegina radiata*). Scale bars in F are 0.1 mm.

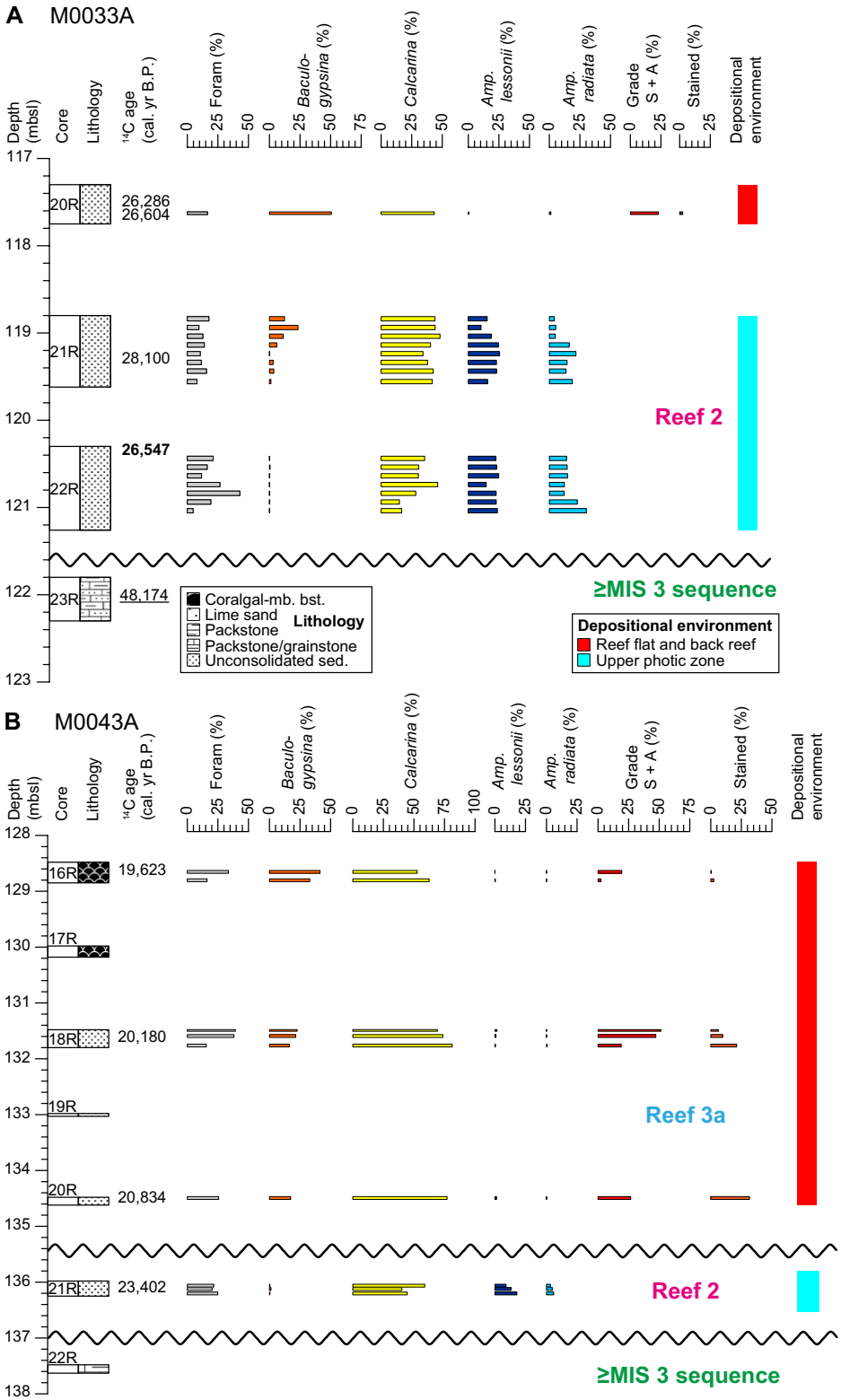

Figure 2. Stratigraphic changes in lithology, radiocarbon (^{14}C, accelerator mass spectrometry) ages (mean; cal. [calibrated] yr B.P.), foraminiferal ("Foram") proportion (percent in 2–0.5 mm grain-size fraction), proportions (in percent) of four key foraminiferal taxa (*Baculogypsina sphaerulata*, *Calcarina* spp., *Amphistegina lessonii*, and *Amphistegina radiata*), proportions (in percent) of taphonomic grades S plus A ("Grade S + A"; see text) and stained tests ("Stained") of *Baculogypsina sphaerulata*, and depositional environments inferred from foraminiferal data set at Integrated Ocean Drilling Project Expedition 325 Holes M0033A (19.6789°S, 150.2399°E, 92.00 m below sea level [mbsl]) (A) and M0043A (19.7963°S, 150.4815°E, 131.27 mbsl) (B), Great Barrier Reef. Bold and underlined numbers in ^{14}C ages represent coral ages by U-Th and ^{14}C dating, respectively (Yokoyama et al., 2018). Undulating line indicates the boundary between reef sequences. See caption of Figure 1 for abbreviations used in the lithology legend. MIS—Marine Isotope Stage.

$\Delta R = 12 \pm 6$ yr was used as the local reservoir correction of the Great Barrier Reef. Sediment accumulation rates (in millimeters per year) were calculated from a core-depth interval divided by the difference in foraminiferal calibrated mean ages between the nearest two samples.

STRATIGRAPHIC CHANGES IN THE FORAMINIFERAL DATA SET

In the IODP Expedition 325 cores, four benthic foraminiferal assemblages have been delineated by multivariate analyses (Q-mode cluster analysis and non-metric multidimensional scaling; Yagioka et al., 2019). As reported in Yagioka et al. (2019), benthic foraminiferal assemblages in the studied intervals show upward changes from assemblage B to assemblage A (Fig. 2; Figs. DR1–DR2 and Table DR1 in the GSA Data Repository[1]). Assemblage B is characterized by *Amphistegina* spp. and *Calcarina* spp., indicative of an upper photic zone (10–30 m deep) associated with hard substrates, while assemblage A is dominated by *Calcarina* spp. and *B. sphaerulata*, indicative of a back-reef to reef-margin zone (0–10 m deep; Yagioka et al., 2019). Assemblage A appears in a narrow depth range (~117 mbsl) for HYD-01C, but at variable depth (118–138 mbsl) for HYD-02A. At core depths where assemblage A appears, foraminiferal proportion in reef sediments is ~26% (up to 56%), associated with corals (~23%), mollusks (~27%), calcareous algae (~20%), and echinoderms (~2.8%). Well-preserved *B. sphaerulata* tests (grades S and A) are also more common (~18%, up to 56%), and the proportion of stained *B. sphaerulata* tests decreases upward (Fig. 2B). ^{14}C-AMS ages of *B. sphaerulata* and *Calcarina* spp., which indicate the time when these foraminifers were alive (i.e., production age), are mainly concentrated at ca. 27–25 ka for HYD-01C, and 22–19 ka for HYD-02A (Fig. 3). Sediment accumulation rates range from 0.74 to 2.86 mm yr^{-1} for HYD-01C, and from 0.61 to 5.28 mm yr^{-1} for HYD-02A (Table DR2). The higher rates correspond to stratigraphic intervals where assemblage A is associated with higher foraminiferal proportions.

EVIDENCE FOR REEF-FLAT AND BACK-REEF FORMATION FOLLOWING LGM RAPID SEA-LEVEL FALLS

Because the basin level change (subsidence) along the northeastern Australia margin has been negligible (0.003–0.05 m k.y.$^{-1}$; Webster et al., 2018), the upward shallowing indicated by foraminiferal assemblages (Yagioka et al., 2019) is likely associated with RSL fall and/or sediment

[1]GSA Data Repository item 2020009, Figures DR1 and DR2, and Tables DR1 and DR2, is available online at http://www.geosociety.org/datarepository/2020/, or on request from editing@geosociety.org.

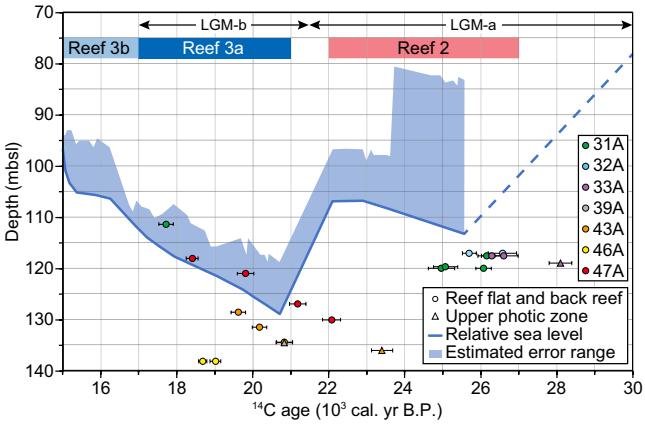

Figure 3. Age-depth plot of foraminiferal tests in comparison with depositional environments inferred from foraminiferal data set and relative sea-level curve at Hydrographers Passage, Great Barrier Reef shown by Yokoyama et al. (2018, detailed and original age data sources therein). Horizontal bars represent 2σ error range. LGM—Last Glacial Maximum; mbsl—meters below sea level.

accumulation. Assemblage A dominated by *Calcarina* spp. and *B. sphaerulata* corresponds to the present-day reef-flat and back-reef assemblages in the Great Barrier Reef (e.g., Doo et al., 2016; Fellowes et al., 2016). High foraminiferal proportions in reef sediments are also similar to those in modern reef-flat sediments (~30%, up to 60%; Yamano et al., 2000; Dawson et al., 2014; Fellowes et al., 2016). Similar proportions of well-preserved *B. sphaerulata* tests are found in the offshore part (e.g., algal turf zone) of modern reef flats (Dawson et al., 2014; Fellowes et al., 2016), indicating that the depositional setting is close to a reef-margin environment. Decreased proportions of stained *B. sphaerulata* tests suggest that most of foraminiferal tests are produced near the depositional setting. Taken together, this evidence implies that reef-flat and back-reef environments were formed during the growth of two distinct reef sequences, which correspond to ca. 27–25 ka (reef 2 in Figs. 1 and 2) for HYD-01C, and 22–19 ka (reef 3a) for HYD-02A, based on our foraminiferal production ages and other published data (Webster et al., 2018; Humblet et al., 2019).

The timing of reef-flat and back-reef formation is consistent with the two stepwise falls in sea level during the LGM (Yokoyama et al., 2018; Fig. 3). Our foraminiferal data set also supports the results of Yokoyama et al. (2018) regarding the nature of sea-level changes during the LGM. The first phase of reef-flat and back-reef formation at ca. 27–25 ka occurred after an initial rapid fall in sea level (>40 m) from 31 to 29 ka (the start of LGM-a period; Lambeck et al., 2014). RSL at Hydrographers Passage was ~110 m at 26 ka then gradually rising afterward to the end of the LGM-a period (21.5 ka; Yokoyama et al., 2018). In response to this initial RSL fall, reef 2 started to grow on Marine Isotope Stage 3 or older slope deposits at ca. 27 ka, forming a very narrow and ephemeral fringing reef system with a slow vertical accretion rate (0.3–2.5 mm yr^{-1}; Webster et al., 2018). Reef flat and back-reef lagoon likely developed as shallow-water reefs accreted to reach sea level, and gradually filled the accommodation space behind the narrow fringing reef system (Fig. 4).

The second phase of reef-flat and back-reef formation at ca. 22–19 ka corresponded to a period following a rapid sea-level fall of ~20 m at ca. 21.5 ka (the start of the LGM-b period; Yokoyama et al., 2018). This sea-level fall resulted in the turn-off (emergent give-up) of reef 2 and the turn-on of reef 3a. Reef 3a migrated seaward within 2 k.y., showing a pattern of shallowing, offlapping sequences (Webster et al., 2018). Reef-flat and back-reef environments likely developed soon after the rapid sea-level fall but also persisted following rising sea levels as reefs accreted and filled the accommodation space behind them. This is supported by a recent reconstruction of the early and rapid deglaciation in the southern-central Great Barrier Reef including Hydrographers Passage, which resulted in a linear, laterally connected coast (Hinestrosa et al., 2019).

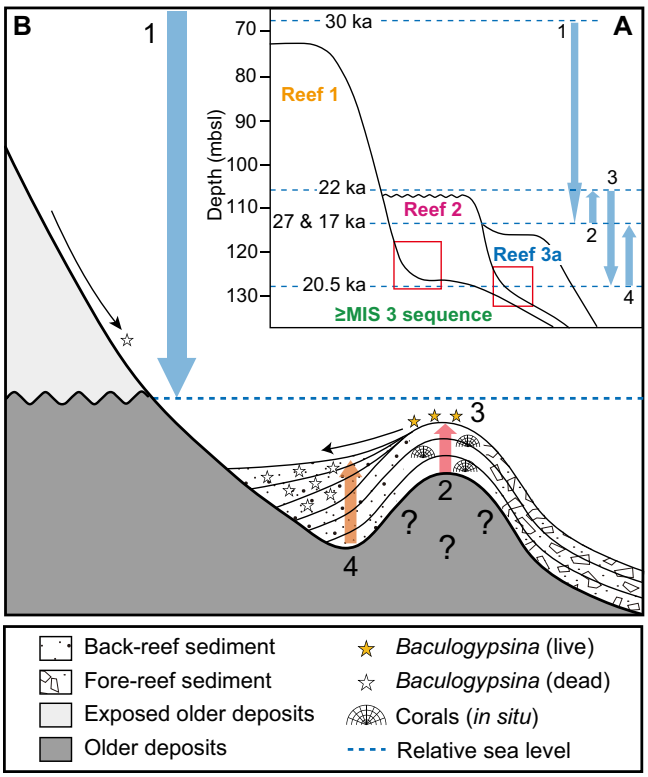

Figure 4. Simplified models of positions of relative sea level (RSL) and reef sequences (A) and of reef-flat and back-reef developments at Hydrographers Passage, Great Barrier Reef, following rapid sea-level falls (B) during the Last Glacial Maximum (LGM). Numbers in A show the order of RSL changes. Red squares indicate positions showing model B. Numbers in B: 1—rapid sea-level fall (early period of both LGM-a and LGM-b) and subaerial exposure of previous reef and associated deposits; 2—reef accretion on preexisting sedimentary structures; 3—reef-flat formation and increasing foraminiferal production; 4—back-reef infilling by reef-flat sediments (foraminiferal tests). Not to scale. mbsl—meters below sea level; MIS—Marine Isotope Stage.

LGM REEF GROWTH AND BACK-REEF SEDIMENTATION

The vertical reef accretion followed by reef-flat and back-reef formation is similar to numerous reefs changing from catch-up to keep-up mode during sea-level rise, relocating in a coastal direction (Woodroffe and Webster, 2014; Camoin and Webster, 2015). However, the driver for LGM reef growth was rapid sea-level fall, and the reef migration was in a seaward position. In addition, antecedent topography may have an important role in how reefs develop during periods of rapid sea-level fall. Geomorphically mature fringing reefs likely developed on preexisting sedimentary structures with a topographic relief (Fig. 4).

Sediment accumulation rates of back-reef deposits following LGM rapid sea-level falls were <5 mm yr^{-1}, which are comparable to or higher than vertical accumulation rates of Holocene back-reef lagoon deposits (<3 mm yr^{-1} on average for the Great Barrier Reef: Montaggioni, 2005; Harris et al., 2015; <7 mm yr^{-1} on average for other regions: e.g., Montaggioni, 2005; Klostermann and Gischler, 2014; Gischler and Kuhn, 2018). This result, together with rare age reversals and commonly well-preserved foraminiferal tests, implies that sufficient accommodation space was available to facilitate the rapid filling and preservation of back-reef sediments following LGM rapid sea-level falls. It might also imply that biological carbonate production may have outpaced that

during the Holocene and previous interglacial periods. Higher carbonate productivity is likely due to relatively high carbonate saturation state and milder sea-surface temperature during the LGM compared to the Holocene and interglacial periods (Felis et al., 2014; Riding et al., 2014).

CONCLUSION

This independent foraminiferal data set supports Yokoyama et al. (2018) in defining the nature of RSL changes in the Great Barrier Reef region during the LGM, while also providing evidence of geomorphically mature fringing reefs during the LGM. We find that antecedent topography likely plays an important role in how reefs develop during periods of rapid sea-level fall. Significantly, the rates of back-reef sediment accumulation were similar or higher during the LGM compared to today.

ACKNOWLEDGMENTS

This research used samples and data provided by IODP. This work was supported by the Japan Society for the Promotion of Science (JSPS) Researcher Exchange Program (FY2015), JSPS KAKENHI grants JP22740339, JP25242026, JP16H02940, JP16H06309, and Australian Research Council Discovery (ARCD) grant DP1094001. We thank Mayuko Ito for help in ^{14}C-AMS measurements. We thank Mick O'Leary and two anonymous reviewers for their constructive comments on the manuscript.

REFERENCES CITED

Braga, J.C., Puga-Bernabéu, Á., Heindel, K., Patterson, M.A., Birgel, D., Peckmann, J., Sánchez-Almazo, I.M., Webster, J.M., Yokoyama, Y., and Riding, R., 2019, Microbialites in Last Glacial Maximum and deglacial reefs of the Great Barrier Reef (IODP Expedition 325, NE Australia): Palaeogeography, Palaeoclimatology, Palaeoecology, v. 514, p. 1–17, https://doi.org/10.1016/j.palaeo.2018.10.007.

Camoin, G.F., and Webster, J.M., 2015, Coral reef response to Quaternary sea-level and environmental changes: State of the science: Sedimentology, v. 62, p. 401–428, https://doi.org/10.1111/sed.12184.

Camoin, G.F., et al., 2012, Reef response to sea-level and environmental changes during the last deglaciation: Integrated Ocean Drilling Program Expedition 310, Tahiti Sea Level: Geology, v. 40, p. 643–646, https://doi.org/10.1130/G32057.1.

Dawson, J.L., Smithers, S.G., and Hua, Q., 2014, The importance of large benthic foraminifera to reef island sediment budget and dynamics at Raine Island, northern Great Barrier Reef: Geomorphology, v. 222, p. 68–81, https://doi.org/10.1016/j.geomorph.2014.03.023.

Doo, S.S., Hamylton, S., Finfer, J., and Byrne, M., 2016, Spatial and temporal variation in reef-scale carbonate storage of large benthic foraminifera: A case study on One Tree Reef: Coral Reefs, v. 36, p. 293–303, https://doi.org/10.1007/s00338-016-1506-0.

Esat, T.M., and Yokoyama, Y., 2006, Growth patterns of the last ice age coral terraces at Huon Peninsula: Global and Planetary Change, v. 54, p. 216–224, https://doi.org/10.1016/j.gloplacha.2006.06.020.

Felis, T., et al., 2014, Intensification of the meridional temperature gradient in the Great Barrier Reef following the Last Glacial Maximum: Nature Communications, v. 5, 4102, https://doi.org/10.1038/ncomms5102.

Fellowes, T.E., Gacutan, J., Harris, D.L., Vila-Concejo, A., Webster, J.M., and Byrne, M., 2016, Patterns of sediment transport using foraminifera tracers across sand aprons on the Great Barrier Reef: Journal of Coastal Research, v. 33, p. 864–873, https://doi.org/10.2112/JCOASTRES-D-16-00082.1.

Gischler, E., and Kuhn, G., 2018, Anatomy of the Holocene inundation of an isolated carbonate platform: Bermuda North Lagoon, western Atlantic: The Depositional Record, v. 4, p. 216–254, https://doi.org/10.1002/dep2.48.

Harris, D.L., Webster, J.M., Vila-Concejo, A., Hua, Q., Yokoyama, Y., and Reimer, P.J., 2015, Late Holocene sea-level fall and turn-off of reef flat carbonate production: Rethinking bucket fill and coral reef growth models: Geology, v. 43, p. 175–178, https://doi.org/10.1130/G35977.1.

Hinestrosa, G., Webster, J.M., and Beaman, R.J., 2016, Postglacial sediment deposition along a mixed carbonate-siliciclastic margin: New constraints from the drowned shelf-edge reefs of the Great Barrier Reef, Australia: Palaeogeography, Palaeoclimatology, Palaeoecology, v. 446, p. 168–185, https://doi.org/10.1016/j.palaeo.2016.01.023.

Hinestrosa, G., Webster, J.M., and Beaman, R.J., 2019, Spatio-temporal patterns in the postglacial flooding of the Great Barrier Reef shelf, Australia: Continental Shelf Research, v. 173, p. 13–26, https://doi.org/10.1016/j.csr.2018.12.001.

Humblet, M., et al., 2019, Late glacial to deglacial variation of coralgal assemblages in the Great Barrier Reef, Australia: Global and Planetary Change, v. 174, p. 70–91, https://doi.org/10.1016/j.gloplacha.2018.12.014.

Kennedy, D.M., and Woodroffe, C.D., 2002, Fringing reef growth and morphology: A review: Earth-Science Reviews, v. 57, p. 255–277, https://doi.org/10.1016/S0012-8252(01)00077-0.

Klostermann, L., and Gischler, E., 2014, Holocene sedimentary evolution of a mid-ocean atoll lagoon, Maldives, Indian Ocean: International Journal of Earth Sciences, v. 104, p. 289–307, https://doi.org/10.1007/s00531-014-1068-8.

Lambeck, K., Rouby, H., Purcell, A., Sun, Y., and Sambridge, M., 2014, Sea level and global ice volumes from the Last Glacial Maximum to the Holocene: Proceedings of the National Academy of Sciences of the United States of America, v. 111, p. 15,296–15,303, https://doi.org/10.1073/pnas.1411762111.

Montaggioni, L.F., 2005, History of Indo-Pacific coral reef systems since the last glaciation: Development patterns and controlling factors: Earth-Science Reviews, v. 71, p. 1–75, https://doi.org/10.1016/j.earscirev.2005.01.002.

Reimer, P.J., et al., 2013, IntCal13 and Marine13 radiocarbon age calibration curves 0–50,000 years cal BP: Radiocarbon, v. 55, p. 1869–1887, https://doi.org/10.2458/azu_js_rc.55.16947.

Riding, R., Liang, L., and Braga, J.C., 2014, Millennial-scale ocean acidification and late Quaternary decline of cryptic bacterial crusts in tropical reefs: Geobiology, v. 12, p. 387–405, https://doi.org/10.1111/gbi.12097.

Sasaki, K., Omura, A., Miwa, T., Tsuji, Y., Matsuda, H., Nakamori, T., Iryu, Y., Yamada, T., Sato, Y., and Nakagawa, H., 2006, ^{230}Th/^{234}U and ^{14}C dating of a lowstand coral reef beneath the insular shelf off Irabu Island, Ryukyus, southwestern Japan: Island Arc, v. 15, p. 455–467, https://doi.org/10.1111/j.1440-1738.2006.00541.x.

Smithers, S., 2011, Fringing reefs, *in* Hopley, D., ed., Encyclopedia of Modern Coral Reefs: Dordrecht, Netherlands, Springer, p. 430–446, https://doi.org/10.1007/978-90-481-2639-2_15.

Webster, J.M., Davies, P.J., and Konishi, K., 1998, Model of fringing reef development in response to progressive sea level fall over the last 7000 years—(Kikai-jima, Ryukyu Islands, Japan): Coral Reefs, v. 17, p. 289–308, https://doi.org/10.1007/s003380050131.

Webster, J.M., et al., 2018, Response of the Great Barrier Reef to sea-level and environmental changes over the past 30,000 years: Nature Geoscience, v. 11, p. 426–432, https://doi.org/10.1038/s41561-018-0127-3.

Woodroffe, C.D., and Webster, J.M., 2014, Coral reefs and sea-level change: Marine Geology, v. 352, p. 248–267, https://doi.org/10.1016/j.margeo.2013.12.006.

Yagioka, N., Nakada, C., Fujita, K., Kan, H., Yokoyama, Y., and Webster, J.M., 2019, Depositional environments beneath the shelf-edge slopes of the Great Barrier Reef, inferred from foraminiferal assemblages: IODP Expedition 325: Palaeogeography, Palaeoclimatology, Palaeoecology, v. 514, p. 386–397, https://doi.org/10.1016/j.palaeo.2018.10.033.

Yamano, H., Miyajima, T., and Koike, I., 2000, Importance of foraminifera for the formation and maintenance of a coral sand cay: Green Island, Australia: Coral Reefs, v. 19, p. 51–58, https://doi.org/10.1007/s003380050226.

Yokoyama, Y., et al., 2018, Rapid glaciation and a two-step sea level plunge into the Last Glacial Maximum: Nature, v. 559, p. 603–607, https://doi.org/10.1038/s41586-018-0335-4.

Yordanova, E.K., and Hohenegger, J., 2002, Taphonomy of larger foraminifera: Relationships between living individuals and empty tests on flat reef slopes (Sesoko Island, Japan): Facies, v. 46, p. 169–203, https://doi.org/10.1007/BF02668080.

Printed in USA